



# Three-dimensional modeling and numerical predictions of multimodal nonlinear behavior in damaged concrete blocks

M. Lott, C. Payan, V. Garnier, P. y Le Bas, T. J Ulrich, M. C Remillieux

## ► To cite this version:

M. Lott, C. Payan, V. Garnier, P. y Le Bas, T. J Ulrich, et al.. Three-dimensional modeling and numerical predictions of multimodal nonlinear behavior in damaged concrete blocks. Journal of the Acoustical Society of America, 2018, 144 (3), pp.1154-1159. 10.1121/1.5053692 . hal-02070844

**HAL Id: hal-02070844**

**<https://hal.science/hal-02070844>**

Submitted on 18 Mar 2019

**HAL** is a multi-disciplinary open access archive for the deposit and dissemination of scientific research documents, whether they are published or not. The documents may come from teaching and research institutions in France or abroad, or from public or private research centers.

L'archive ouverte pluridisciplinaire **HAL**, est destinée au dépôt et à la diffusion de documents scientifiques de niveau recherche, publiés ou non, émanant des établissements d'enseignement et de recherche français ou étrangers, des laboratoires publics ou privés.

**Three-dimensional modeling and numerical predictions of multimodal  
nonlinear behavior in damaged concrete blocks.**

M. Lott<sup>1</sup>, C. Payan<sup>1\*</sup>, V. Garnier<sup>1</sup>, P.Y. Le Bas<sup>2</sup>, T.J. Ulrich<sup>2</sup>, M.C. Remillieux<sup>3</sup>

<sup>1</sup>Aix Marseille Univ, CNRS, Centrale Marseille, LMA, Marseille, France

<sup>2</sup>Detonation Science and Technology Group (Q-6), Los Alamos National Laboratory,  
Los Alamos, New Mexico 87545, USA

<sup>3</sup>Geophysics Group (EES-17), Los Alamos National Laboratory, Los Alamos,  
New Mexico 87545, USA

\*corresponding author: [cedric.payan@univ-amu.fr](mailto:cedric.payan@univ-amu.fr)

**Abstract**

In this paper, the multimodal nonlinear elastic behavior of concrete, which is representative of a consolidated granular material, is modeled numerically. Starting from a local three-dimensional softening law, the initial stiffness properties are re-estimated according to the local strain field. The experiments deal with samples of thermally damaged concrete blocks successively excited around their first three modes of vibration. The geometry of these samples cannot be described by a one-dimensional approximation in these experiments where compressional and shear motions are strongly coupled. Despite this added complexity, the nonlinear behavior for the three modes of vibration of the samples is well captured by the simulations using a single scalar nonlinear parameter appropriately integrated into the elasticity equations. It is shown that without sufficient attention paid to the latter, the conclusions would have brought erroneous statements such as nonlinearity dispersion or strain type dependence.

## I. Introduction

Geomaterials exhibit mechanical softening under dynamic loading, usually combined with hysteresis and slow-dynamics effects (Johnson *et al.*, 1996; TenCate *et al.*, 2000). These effects are reversible and deterministic. From a micro-structure standpoint, a recent study has established a correlation between micro-crack density and softening effects (Payan *et al.*, 2014a,b). From an energy balance point of view, it means that some potential energy disappears when the material is loaded dynamically and is slowly recovered when the material is at rest. These properties are relevant to various natural processes and industrial applications including the onset of earthquake and avalanches in geophysics (Johnson and Jia, 2005), the aging of civil infrastructure (Eiras *et al.*, 2016; Payan *et al.*, 2007; Vu *et al.*, 2016), the design of acoustic meta-materials with extreme stiffness (Diani *et al.*, 2009; Wang and Lakes, 2004), or the assessment of bone fragility in the medical field (Hauptert *et al.*, 2014).

The dynamic response of these materials has been first modeled by Guyer *et al.* (1995) using the Preisach formalism, which is a phenomenological description borrowed from the field of electromagnetics. This model has then been refined to include slow-dynamics effects through thermally activated random transitions between the open and closed states of the hysteretic elements of the Preisach system (Delsanto and Scalerandi, 2003; Nobili and Scalerandi, 2004). More recently, Pecorari (2015) proposed a hysteretic model sharing some features with the Jiles-Atherton model (also borrowed from the field of electromagnetics), which he enhanced to capture the slow-dynamics effects. It is also worth mentioning the soft-ratchet model of slow-dynamics originally proposed by Vakhnenko *et al.* (2004) and recently modified by Favrie *et al.* (2015) to include classical nonlinearity and viscoelasticity. All these models, however, have been derived in the one-dimensional (1D). Three-dimensional (3D) effects are an essential part of the dynamic response observed in geomaterials and cannot be ignored (Egle and Bray, 1976; Payan *et al.*, 2007, 2009; Tournat *et al.*, 2004). Lyakhovsky *et al.* (2009) proposed a two-dimensional continuum damage rheology model capturing hysteretic nonlinearity and some of the features observed in nonlinear resonance experiments. A similar model was used by Hamiel *et al.* (2009) to describe stress-induced anisotropy in damaged geomaterials. Note that in these models, damage is not recoverable and slow-dynamics effects are not considered. The recent modeling work of Berjamin *et al.* (2017) includes slow-dynamics effects, but although it can be naturally extended to 3D analysis, the simulations are carried out only for a 1D case.

Attempting to develop a predictive tool to link the microstructural properties of the material to the nonlinear elastic response observed experimentally is a challenging task. Despite a high sensitivity to microstructures, amorphous condensed matter arrangement, and environmental conditions (e.g., temperature, pressure) (Lott *et al.*, 2016; Payan *et al.*, 2009; TenCate *et al.*, 2000), the elastic nonlinear parameters seem to depend on the choice of the experimental setup in much of the previous work reported in the literature. For instance, Renaud *et al.* (2013) showed that material softening effects in Berea sandstone may vary by up to an order of magnitude depending on the probing direction while the material is isotropic. In the work of Payan *et al.* (2014a,b) on concrete, two techniques were used to estimate a parameter of nonlinearity. The two techniques showed the same trends but the magnitudes of the measured parameter differ by an order of magnitude. These experimental data were derived using the most common 1D approximation. However, a complex strain field leads to a 3D problem from a mechanical point of view and using a 1D approximation to describe this problem may lead to erroneous conclusions.

Recently, Lott *et al.* (2016, 2017) show that conditioning can be properly accounted in 3D using a single scalar nonlinear parameter into the appropriate set of elasticity equations using uncoupled single mode resonance type of experiments, i.e., shear and compressional. The aim of this paper is to study the validity of this model to nonlinear resonance experiments, involving strong coupling between shear and compressional motion types. Numerical simulations are compared to experimental data from nonlinear resonances in gradually thermally damaged concrete blocks. Using a single scalar nonlinear parameter appropriately introduced in elasticity equations, the validity of the model is demonstrated and discussed.

## II. Theoretical framework

In continuum mechanics, the parameters needed to compute the linear dynamic response of an elastic body are the mass density, the linear elastic tensor, and the damping parameters. If the geometry of the sample is complex and/or the material is heterogeneous, numerical techniques (e.g., finite-element method) should be used and the distribution of these parameters should be known for all computation cells discretizing the sample. In this paper, we study consolidated granular materials, which may be described as a disordered network of mesoscopic-sized “hard”

elements (e.g., grains with characteristic lengths ranging from tens to hundreds of microns) cemented together by a “soft” bond system (e.g., amorphous silica, calcite) (Guyer and Johnson, 1999). Despite the complexity of the structure, the linear elastic response of these materials at macroscopic scale is well captured by the model of a continuum. This continuum may have heterogeneous properties under dynamic loading as a combined result of the complex spatio-temporal distribution of the strain field in the sample and the strain-induced material softening (Payan *et al.*, 2007; Remillieux *et al.*, 2015; Renaud *et al.*, 2013). Material softening is thought to originate from the microscopic-sized defects (e.g., micro-cracks) in the “soft” subsystem and at the interfaces between the “hard” and “soft” subsystems (Payan *et al.*, 2014a). To incorporate these defects in the macroscopic continuum model, we consider a volume  $dV$  that is small enough to satisfy the requirements of the numerical schemes but large enough to ensure a constant micro-crack density from one volume to the next. Furthermore, we assume that the defects are randomly distributed and oriented within the volume  $dV$ , with a length-scale much smaller than the typical acoustic wavelengths used in this study. With  $dV$  being on the order of  $1\text{mm}^3$ , the above criteria are satisfied.

The approach used in this paper is similar to the one used by Zubelewicz (1990) in transient numerical simulations of rock fractures. Each contact within the medium brings softening effects through nonlinear cohesive mechanisms. These effects are then integrated over an elementary volume  $dV$  and used for a mesoscopic mechanical implementation within a continuum with possible heterogeneous properties.

Recently, the authors (Lott *et al.*, 2016, 2017) proposed a general formulation to include material-softening effects in the equations of elasticity. This formulation is an extension of that proposed by Hughes and Kelly (Hughes and Kelly, 1953). The tensorial product between the strain and stress vector bases,  $\delta_{ij} = n_i^{stress} \otimes n_j^{strain}$ , is the natural basis for the elastic tensor and should now include softening effects as,

$$\Lambda_{ij} = \delta_{ij} (1 - \alpha \Delta \varepsilon_{ij}^*), \quad (1)$$

or equivalently in matrix form as,

$$\mathbf{\Lambda} = \mathbf{I}_3 - \alpha \mathbf{\varepsilon}^*, \quad (2)$$

where  $n_i$  is the principal strain direction,  $\Delta \varepsilon_{ij}^*$  the strain amplitude, the star symbol denotes the basis formed by the principal strain axes, and  $\alpha$  is a scalar quantifying the softening effect. The stiffness tensor is then expressed as,

$$C_{ijkl}^* = [\lambda + 2(l - \lambda - m)Tr(\varepsilon) + 2(\lambda + m)(\varepsilon_i^* + \varepsilon_k^*) - 2\mu\varepsilon_i]\Lambda_{ij}\Lambda_{kl} + [\mu + (\lambda + m - \mu)Tr(\varepsilon) + 2\mu(\varepsilon_i + \varepsilon_j + \varepsilon_l)](\Lambda_{ik}\Lambda_{jl} + \Lambda_{il}\Lambda_{jk}) + \frac{1}{2}n \sum_v (\Lambda_{jvk}^{ivl} + \Lambda_{jvl}^{ivk})\varepsilon_v \quad (3)$$

where  $\lambda$  and  $\mu$  are the Lamé constants and  $l, m, n$  are the Murnaghan constants (Murnaghan, 1937). Practically, the material-softening law is applied in the basis formed by the principal strain axes. This basis is obtained from an eigen decomposition of the strain field  $\varepsilon$  measured in the geometric basis. This decomposition,  $\varepsilon = \mathbf{P} \varepsilon^* \mathbf{P}^{-1}$ , is always possible because the strain tensor is always real and symmetric. Once the softening law has been applied to the stiffness tensor in the basis formed by the principal strain axes, the following transformation is used to express the conditioned stiffness tensor in the geometric basis:  $C_{ijkl} = P_{ir}P_{js}P_{kt}P_{lu}C_{rstu}^*$ . This result is equivalent to classical acoustoelasticity theory when the term quantifying softening is equal to the identity matrix.

In this study, the validity of the model will be assessed using nonlinear resonance experiments or more commonly referred to in the literature as nonlinear resonant ultrasound spectroscopy (NRUS). In these experiments, a sample is subjected to sequences of periodic signals at various frequencies around a resonance frequency and at increasing amplitudes while, for each periodic signal, data are recorded when the sample vibrates at or near a steady state. Under these conditions, the effects of the first-order term of nonlinearity in the classical description, i.e., terms involving  $\beta$  in 1D and  $(l, m, n)$  in 3D, average to zero over one cycle of the harmonic excitation. This is not the case with the second-order term of nonlinearity  $\delta$  but the proposed model does not go beyond the first order. As a result, Eq. (3) can be simplified by removing the terms involving third-order elastic constants (i.e., only the linear version of the elastic tensor is used to apply the softening law),

$$C_{ijkl}^* = \lambda \Lambda_{ij}\Lambda_{kl} + \mu (\Lambda_{ik}\Lambda_{jl} + \Lambda_{il}\Lambda_{jk}). \quad (4)$$

Finally, each cell (dV) of the sample can be conditioned by the strain amplitude at that cell. This means that the stiffness tensor is no longer uniform over the volume of the sample but depends on the local strain tensor. The sample experiences softening with a complex distribution (i.e., that of the strain field), which in turns lowers its resonance frequencies. Because of the heterogeneity, the resonance frequencies have to be computed numerically.

### III. Numerical application to experimental data

The validity of the model is examined against experimental data collected during resonance experiments. The samples are those described by Payan et al. (2014b). The three samples used in this study consist of concrete blocks with dimensions  $6 \times 10 \times 10 \text{ cm}^3$ . One sample is kept intact and used as a reference. The other two samples are thermally damaged at 120 and at 250°C using a slow increase then decrease in temperature to prevent from eventual mechanical damage induced by thermal gradients. Thermal damage allows the density of micro-cracking within the concrete samples to be increased as needed. Below 300° C, microcracks are essentially caused by drying as well as differential thermal dilatation between cement paste and aggregates. In concrete the most brittle zone is the interface between the aggregates and the cement paste. This zone, commonly referred to as Interfacial Transition Zone (ITZ), is the most porous and crystallized region. It is thus quite natural to assume that most of the thermal damage will occur in the ITZ. With an arbitrary grain distribution, thermal damage of concrete can reasonably be considered as isotropic.

#### A. Experimental protocol and results

The samples are excited with an ultrasonic cleaning transducer (Ultrasonics World, DE, USA) powered by a function generator (National Instrument PXI-5406 function generator) coupled to a voltage amplifier (TEGAM 2350). The vibrational responses of the samples are recorded by a Polytec laser vibrometer (OFV 5000, 1.5 MHz bandwidth) using a digitizer (National Instrument PXI-5122). Both generation and acquisition lines are managed by the NRUS module of the Resonance Inspection Techniques and Analysis (RITA) software designed and implemented by T. J. Ulrich and Pierre-Yves Le Bas at Los Alamos National Laboratory. More

details about the signal processing for these experiments may be found in the paper of Payan et al. (2014b).

Three resonant modes are then considered for NRUS. The mode shapes, source, and receiver positions are shown in Fig.1 for the sample thermally damaged at 120°C. Two of the modes are dominated by a bending motion and require the source and receiver to be located near the corners of the sample, where the amplitude is the highest, to enhance the signal to noise ratio. The third mode studied here consists of a “bulk/breathing” motion which is excited by placing the source transducer at the center of one large face and recorded by pointing the laser beam at the center of the opposite face.

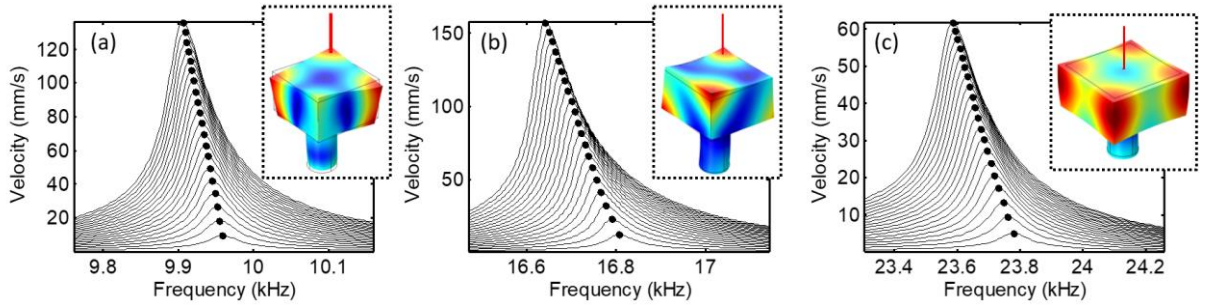


FIG. 1. (Color online) Experimental (a) first, (b) second and (c) third NRUS curves for the 120°C damaged sample. Insets are the corresponding modal shapes.

## B. Numerical protocol

The relatively large mass added by the transducer is accounted for in the model by an aluminum cylinder with a perfect contact between the transducer and the sample. The following protocol is applied (Fig.2) to describe the numerical process. The simulations are carried out using the “Structural Mechanics” module of the commercial finite-element software package Comsol® Multiphysics.

- Step 1 : A first eigenvalue problem is solved to compute the resonance frequencies of the samples with linear elastic properties (before the material-softening law is applied), which were already measured by Payan *et al.* (2014b) in previous work. The predicted and measured resonance frequencies of the systems with linear elastic properties that are reported in Table. I are in excellent agreement. Having a representative and accurate linear model is essential to the numerical protocol in this problem because the maximum values

of strain amplitudes in the samples are recovered from the linear model, based on the laser measurement at a single point.

- Step 2 : In the second step of the numerical protocol, a frequency-domain simulation is conducted by imposing a normal force on the free flat surface where the transducer is mounted. The amplitude of the normal force is tuned to match the particle velocity at the measured position on the sample.
- Step 3 (Fig.2) : The strain tensor is extracted at all nodes of the mesh discretizing the sample and used for the conditioning step. As the media is initially considered isotropic and homogeneous, the initial local stiffness is independent of the choice of basis and usually written  $C_{ijkl} = \lambda \delta_{ij}\delta_{kl} + \mu (\delta_{ik}\delta_{jl} + \delta_{il}\delta_{jk})$ . Using Eq. (1) and Eq. (4), the material softening effect is applied to the stiffness tensor  $C_{ijkl}^*$  through the tensors  $\Lambda_{ij}$  in the eigen basis.
- Step 4 (Fig.2) : The conditioned elastic tensor is then transposed back to the “geometrical” basis. After this numerical procedure, the sample, initially homogeneous and isotropic, becomes heterogeneous and anisotropic.
- Step 5 : A final eigenvalue problem is solved to compute the resonance frequencies of the samples with conditioned elastic properties. Steps 2 to 5 are repeated for several amplitudes to provide a curve of the relative shift of the resonance frequency.

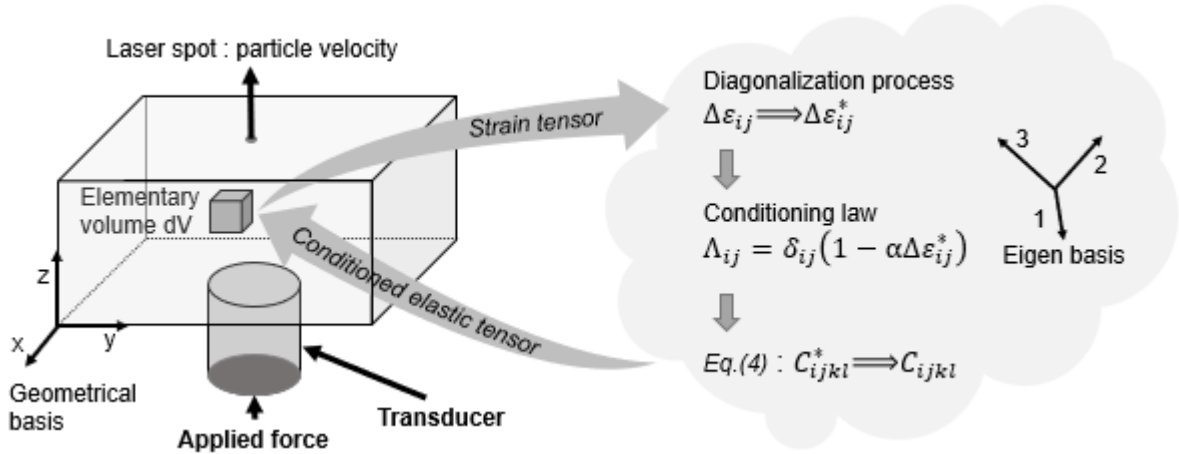


FIG. 2. Scheme of the numerical and experimental protocols.

Resonance frequencies $f_0$ (kHz)						
Sample	Mode 1		Mode 2		Mode 3	
	Exp	Num	Exp	Num	Exp	Num
Ref	10.16	10.09 (-0.7%)	17.33	17.36 (+0.2%)	24.02	24.43(+1.7%)

120°C	9.95	9.96 (+0.1%)	16.86	16.81 (-0.3%)	23.30	23.79 (+2.1%)
250°C	9.43	9.53 (+1%)	15.97	14.739 (-7.7%)	22.31	22.30 (-0.1%)

Table. I. Resonance frequencies obtained experimentally and numerically with linear RUS.

#### IV. Results and discussion

Predicted and measured material softening in NRUS are shown in Fig.3 for the three samples. The values of  $\alpha_0$  used in the simulations to match the experimental data are reported in Table.

II.

Sample	$\alpha_0$
Reference	300
120°C	520
250°C	1000

Table. II. Values of the parameter  $\alpha_0$  used in the NRUS simulations for the three concrete samples.

Note that this value increases by more than 300% between the reference sample and the most damaged sample, which seems to be consistent with the evolutions of the nonlinear parameters reported in the literature. To highlight the efficiency of the present model, the “apparent” nonlinear parameters are measured by linear regression of the relative frequency shift as a function of the strain amplitude for the three modes studied. This apparent nonlinear parameter changes with the mode order and the type of strain (e.g., volumetric and deviatoric) used in the analysis. For each mode and each sample, the apparent nonlinear parameters obtained with volumetric and deviatoric strains are reported in Fig.4. Tying this apparent nonlinear parameter to a 1D description will lead to erroneous conclusions including that the nonlinearity is dispersive (i.e., depends on the order of the mode) or is dependent on the type of strain involved (e.g., shear or compressional components). It is important to stress that the nonclassical nonlinearity should be handled by a local parameter appropriately integrated within the elasticity equations.

Numerical simulations using a single scalar parameter  $\alpha_0$  reproduce well the experimental observations, independently from the type of strain used or the mode order employed in the

1 nonlinear analysis. There are some discrepancies between numerical simulation and  
2 experiments for some cases, but it does not seem to be consistent with the type of mode or a  
3 particular sample. Discrepancies are most likely due to the complexity of the experiment and  
4 the presence of a large transducer mounted at various positions on the sample to excite the  
5 various modes. Also, the sample do not have the perfect parallelepiped geometry used in the  
6 model. Even if the sample size was precisely measured using a caliper, parallelisms deviations  
7 are not accounted for in the simulations.

8  
9 For the third mode, all the frequency shifts flatten a little bit at increasing amplitude (Fig.3).  
10 This behavior may be induced by some hidden resonant peaks which could appear at high  
11 amplitude. This can happen especially at “high” frequency when the resonance frequency  
12 density becomes high. Even if the location of the transducer was chosen so as to favor a given  
13 mode shape, other nearby resonances may alter these curves.

14  
15 More importantly, the simulation results indicate that, in the case of concrete the nonlinear  
16 behavior of the material for both compressional and torsional motions is well captured by a  
17 single local scalar parameter. These results are in agreement with the fact that the distribution  
18 of defects in the thermally damaged concrete samples is isotropic.

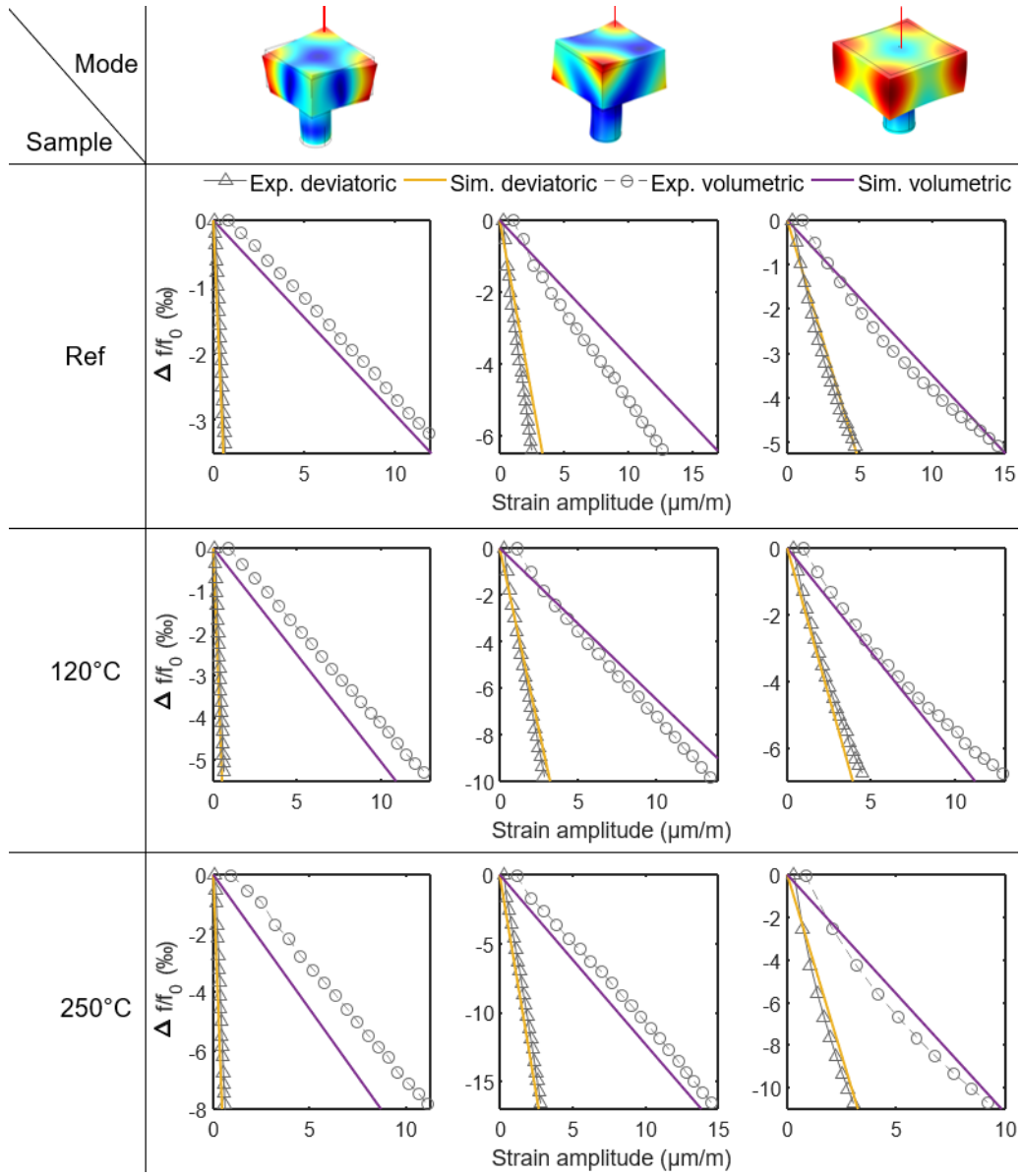


FIG. 3. (Color online) Experimental and numerically predicted resonances curves for the whole set of samples and modal shapes.

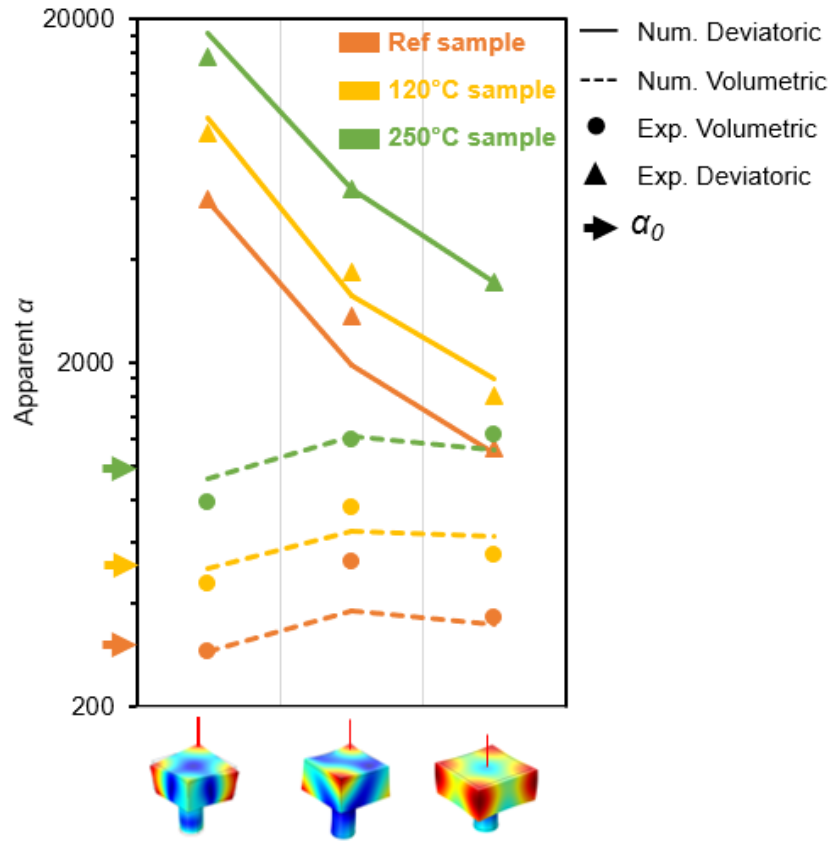


FIG. 4. (Color online) Experimental and numerically derived apparent nonlinear parameters.  $\alpha_0$  is also reported for comparison.

## V. Conclusion

A tensorial interpretation of the softening effects under dynamic stress was integrated in a numerical scheme using a single scalar parameter. The key feature of the model relies on locally applying a softening law to the elastic tensor in the eigenbasis of the strain field and transforming this tensor back to the geometrical basis once the softening has been applied. Numerical simulation results were compared to nonlinear multi-modal resonance experiments on thermally damaged concrete samples. In these samples, it was well adapted to predicting nonlinear behavior of their complex mode shapes involving coupling between shear and compressional components. This is in good agreement with the fact that an isotropic distribution of defects is expected in these materials.

It also shown that without accounting for these issues, the derived apparent nonlinear parameter can lead to erroneous interpretations. In this study, one could conclude to frequency dispersion

or strain type dependences of nonlinearity. However, none of these statements are supported by the appropriate description of nonlinearity in the elasticity equations.

Future improvements of the model will aim at accounting for textured type of microcracking using the more general framework of a vectorial nonlinear parameter. Indeed, experimental data reported in the literature (Remillieux *et al.* 2016; Lott *et al.* 2017) show that many sedimentary rocks (e.g., Berea sandstone) exhibiting preferred oriented micro cracking features would require such a description.

## Acknowledgments

This work was supported by the French National Research Agency through the ENDE program (Grant No. ANR-11 RSNR 0009) and the U.S. Department of Energy through the Fossil Energy program (Grant No. FE-634-15-FY15).

## References

- Berjamin, H., Favrie, N., Lombard, B., and Chiavassa, G. (2017). "Nonlinear waves in solids with slow dynamics: an internal-variable model," in Proc. R. Soc. A, The Royal Society, Vol. 473, p. 20170024.
- Delsanto, P. P., and Scalerandi, M. (2003). "Modeling nonclassical nonlinearity, conditioning, and slow dynamics effects in mesoscopic elastic materials," Physical Review B 68(6), 350 064107.
- Diani, J., Fayolle, B., and Gilormini, P. (2009). "A review on the mullins effect," European Polymer Journal 45(3), 601–612.
- Egle, D. M., and Bray, D. E. (1976). "Measurement of acoustoelastic and third-order elastic constants for rail steel," The journal of the Acoustical Society of America 60(3), 741–744.
- Eiras, J. N., Vu, Q. A., Lott, M., Paya, J., Garnier, V., and Payan, C. (2016). "Dynamic acousto-elastic test using continuous probe wave and transient vibration to investigate material nonlinearity," Ultrasonics 69, 29–37.

- 1 Favrie, N., Lombard, B., and Payan, C. **(2015)**. “Fast and slow dynamics in a nonlinear elastic  
2 bar excited by longitudinal vibrations,” *Wave Motion* 56, 221–238.
- 3
- 4 Guyer, R. A., and Johnson, P. A. **(1999)**. “Nonlinear mesoscopic elasticity: Evidence for a new  
5 class of materials,” *Physics today* 52, 30–36.
- 6
- 7 Guyer, R. A., McCall, K. R., and Boitnott, G. N. **(1995)**. “Hysteresis, discrete memory, and  
8 nonlinear wave propagation in rock: A new paradigm,” *Physical Review Letters* 74(17), 3491.
- 9
- 10 Hamiel, Y., Lyakhovsky, V., Stanchits, S., Dresen, G., and Ben-Zion, Y. **(2009)**. “Brittle  
11 deformation and damage-induced seismic wave anisotropy in rocks,” *Geophysical Journal*  
12 *International* 178(2), 901–909.
- 13
- 14 Hauptert, S., Guerard, S., Peyrin, F., Mitton, D., and Laugier, P. **(2014)**. “Non destructive  
15 characterization of cortical bone micro-damage by nonlinear resonant ultrasound  
16 spectroscopy,” *PLoS One* 9(1), e83599.
- 17 Hughes, D. S., and Kelly, J. L. **(1953)**. “Second-order elastic deformation of solids,” *Physical*  
18 *review* 92(5), 1145.
- 19
- 20 Johnson, P. A., and Jia, X. **(2005)**. “Nonlinear dynamics, granular media and dynamic  
21 earthquake triggering,” *Nature* 437(7060), 871.
- 22
- 23 Johnson, P. A., Zinszner, B., and Rasolofosaon, P. N. **(1996)**. “Resonance and elastic nonlinear  
24 phenomena in rock,” *Journal of Geophysical Research: Solid Earth* 101(B5), 11553–11564.
- 25
- 26 Lott, M., Payan, C., Garnier, V., Vu, Q. A., Eiras, J. N., Remillieux, M. C., Le Bas, P.-Y., and  
27 Ulrich, T. J. **(2016)**. “Three-dimensional treatment of nonequilibrium dynamics and higher  
28 order elasticity,” *Applied Physics Letters* 108(14), 141907.
- 29
- 30 Lott, M., Remillieux, M. C., Garnier, V., Le Bas, P.-Y., Ulrich, T. J., and Payan, C. **(2017)**.  
31 “Nonlinear elasticity in rocks: A comprehensive three-dimensional description,” *Physical*  
32 *Review Materials* 1(2), 023603.
- 33

- 1 Lyakhovsky, V., Hamiel, Y., Ampuero, J.-P., and Ben-Zion, Y. **(2009)**. “Non-linear damage  
2 rheology and wave resonance in rocks,” *Geophysical Journal International* 178(2), 910–920.  
3
- 4 Murnaghan, F. D. (1937). “Finite deformations of an elastic solid,” *American Journal of*  
5 *Mathematics* 59(2), 235–260.  
6
- 7 Nobili, M., and Scalerandi, M. **(2004)**. “Temperature effects on the elastic properties of  
8 hysteretic elastic media: Modeling and simulations,” *Physical Review B* 69(10), 104105.  
9
- 10 Pasqualini, D., Heitmann, K., TenCate, J. A., Habib, S., Higdon, D., and Johnson, P. A. **(2007)**.  
11 “Nonequilibrium and nonlinear dynamics in berea and fontainebleau sandstones: Low-strain  
12 regime,” *Journal of Geophysical Research: Solid Earth* 112(B1).  
13
- 14 Payan, C., Garnier, V., Moysan, J., and Johnson, P. A. **(2007)**. “Applying nonlinear resonant  
15 ultrasound spectroscopy to improving thermal damage assessment in concrete,” *The Journal of*  
16 *the Acoustical Society of America* 121(4), EL125–EL130.  
17
- 18 Payan, C., Garnier, V., Moysan, J., and Johnson, P. A. **(2009)**. “Determination of third order  
19 elastic constants in a complex solid applying coda wave interferometry,” *Applied Physics*  
20 *Letters* 94(1), 011904.  
21
- 22 Payan, C., Ulrich, T. J., Le Bas, P. Y., Griffo, M., Schuetz, P., Remillieux, M. C., and Saleh, T.  
23 A. **(2014a)**. “Probing material nonlinearity at various depths by time reversal mirrors,” *Applied*  
24 *Physics Letters* 104(14), 144102.  
25
- 26 Payan, C., Ulrich, T. J., Le Bas, P. Y., Saleh, T., and Guimaraes, M. **(2014b)**. “Quantitative  
27 linear and nonlinear resonance inspection techniques and analysis for material characterization:  
28 Application to concrete thermal damage,” *The Journal of the Acoustical Society of America*  
29 136(2), 537–546.  
30
- 31 Pecorari, C. **(2015)**. “A constitutive relationship for mechanical hysteresis of sandstone  
32 materials,” in *Proc. R. Soc. A, The Royal Society*, Vol. 471, p. 20150369.  
33

- 1 Remillieux, M. C., Guyer, R. A., Payan, C., and Ulrich, T. J. **(2016)**. “Decoupling nonclassical  
2 nonlinear behavior of elastic wave types,” *Physical review letters* 116(11), 115501.
- 3
- 4 Remillieux, M. C., Ulrich, T. J., Payan, C., Rivière, J., Lake, C. R., and Le Bas, P.-Y. **(2015)**.  
5 “Resonant ultrasound spectroscopy for materials with high damping and samples of arbitrary  
6 geometry,” *Journal of Geophysical Research: Solid Earth* 120(7), 4898–4916.
- 7
- 8 Renaud, G., Rivière, J., Hauptert, S., and Laugier, P. **(2013)**. “Anisotropy of dynamic  
9 acoustoelasticity in limestone, influence of conditioning, and comparison with nonlinear  
10 resonance spectroscopy,” *The Journal of the Acoustical Society of America* 133(6), 3706–3718.
- 11
- 12 TenCate, J. A., Pasqualini, D., Habib, S., Heitmann, K., Higdon, D., and Johnson, P. A. **(2004)**.  
13 “Nonlinear and nonequilibrium dynamics in geomaterials,” *Physical review letters* 93(6),  
14 065501.
- 15
- 16 Tournat, V., Zaitsev, V., Gusev, V., Nazarov, V., Béquin, P., and Castagnede, B. **(2004)**.  
17 “Probing weak forces in granular media through nonlinear dynamic dilatancy: clapping  
18 contacts and polarization anisotropy,” *Physical review letters* 92(8), 085502.
- 19
- 20 Vakhnenko, O. O., Vakhnenko, V. O., Shankland, T. J., and Ten Cate, J. A. **(2004)**. “Strain  
21 induced kinetics of intergrain defects as the mechanism of slow dynamics in the nonlinear  
22 resonant response of humid sandstone bars,” *Physical Review E* 70(1), 015602.
- 23
- 24 Vu, Q. A., Garnier, V., Chaix, J. F., Payan, C., Lott, M., and Eiras, J. N. **(2016)**. “Concrete  
25 cover characterisation using dynamic acousto-elastic testing and rayleigh waves,” *Construction  
26 and Building Materials* 114, 87–97.
- 27
- 28 Wang, Y. C., and Lakes, R. S. **(2004)**. “Extreme stiffness systems due to negative stiffness  
29 elements,” *American Journal of Physics* 72(1), 40–50.
- 30
- 31 Zubelewicz, A. **(1990)**. “Overall stress and strain rates for crystalline and frictional materials,”  
32 *International Journal of Non-Linear Mechanics* 25(4), 389–393.
- 33

# TABLES

Resonance frequencies $f_0$ (kHz)						
Sample	Mode 1		Mode 2		Mode 3	
	Exp	Num	Exp	Num	Exp	Num
Ref	10.16	10.09 (-0.7%)	17.33	17.36 (+0.2%)	24.02	24.43(+1.7%)
120°C	9.95	9.96 (+0.1%)	16.86	16.81 (-0.3%)	23.30	23.79 (+2.1%)
250°C	9.43	9.53 (+1%)	15.97	14.739 (-7.7%)	22.31	22.30 (-0.1%)

Table. I. Resonance frequencies obtained experimentally and numerically with linear RUS.

Sample	$\alpha_0$
Reference	300
120°C	520
250°C	1000

Table. II. Values of the parameter  $\alpha_0$  used in the NRUS simulations for the three concrete samples.

**FIGURE CAPTION**

FIG. 1. (Color online) Experimental (a) first, (b) second and (c) third NRUS curves for the 120°C damaged sample. Insets are the corresponding modal shapes.

FIG. 2. Scheme of the numerical and experimental protocols.

FIG. 3. (Color online) Experimental and numerically predicted resonances curves for the whole set of samples and modal shapes.

FIG. 4. (Color online) Experimental and numerically derived apparent nonlinear parameters.  $\alpha_0$  is also reported for comparison.